Near-bed turbulence dynamics and suspended sediment transport over mixed sand-clay substrates

Xuxu Wu *University of Hull, Hull, U.K. – x.wu@hull.ac.uk*
Daniel Parsons *University of Hull, Hull, U.K. – d.parsons@hull.ac.uk*
Jaco H. Baas *Bangor University, Bangor, U.K. – d.parsons@hull.ac.uk*
Dominique Mouazé *University of Caen, Caen, France – dominique.mouaze@unicaen.fr*
Stuart McLelland *University of Hull, Hull, U.K. – s.j.mclelland@hull.ac.uk*
Laurent Amoudry *National Oceanography Centre, Liverpool, U.K. – laou@noc.ac.uk*
Jorris Eggenhuisen *University of Utrecht, Utrecht, Netherlands. – j.t.eggenhuisen@uu.nl*
Matthieu Cartigny*, Durham University, Durham, U.K.. – matthieu.j.cartigny@durham.ac.uk*
Gerben Ruessink *University of Utrecht, Utrecht, Netherlands. – b.g.ruessink@uu.nl*

ABSTRACT: This paper reports on a series of experiments that aim to provide a fuller understanding of ripple development within clay-sand mixture substrates under oscillatory flow conditions. The work was conducted in the Total Environment Simulator at the University of Hull and constituted 5 separate runs. The bed content was systematically varied in its composition ranging from a pure sand bed through to a bed comprising 7.4% clay. A series of state-of-the-art measurements were employed to quantify interactions of near-bed hydrodynamics, sediment transport, and turbulence over rippled beds formed by wave action, during and after, each run. The experimental results demonstrate the significant influence of the amount of cohesive clay materials in the substrate on sediment transport. Most importantly, the time averaged suspended sediment concentration (SSC) at height of 20 mm above bed significantly increased from the flat bed evolving to equilibrium wave ripples. Additionally, the clay remaining in the bed is able to stabilize the rippled bed by significantly decreasing ripple migration rate from 0.14 mm/s in Run 1 to 0.04 mm/s in Run 6.

1 INTRODUCTION

Sediment transport, which includes bed-load and near-bed suspended load, is a dynamic process closely related to hydrodynamic forcing, turbulence, and bed substrate properties (Leeder, 2011). It directly contributes to bedform formation (e.g., ripples). In coastal environments, wave-induced turbulence over flat beds and the spatially and temporally generated vortex on the ripple lee side during oscillatory flow reversal (Ikeda et al., 1991) largely results in suspended sediments, dominating sediment transport (Nielsen, 1992). Although a number of flume and field investigations have previously studied sediment transport and morphodynamics under oscillatory flows (e.g., Green & Black, 1999), the co-evolution of the bed morphology and oscillatory flow structures have only been examined for cases of cohesionless sand substrates (e.g., van der Werf et al., 2007; O’Hara Murray et al., 2011). There is thus a significant knowledge gap concerning the influence of substrate cohesiveness on sediment transport and bedform generation.

The development rate of wave ripple dramatically decreases with initial bed clay fraction increase (Wu et al., 2018). The increasing bed resistance related to the initial bed clay fraction plays a vital role on slowing wave-induced ripple development. In the present paper, near-bed wave-generated turbulence and sediment transport dynamics are investigated over the evolving substrates. The objectives of this paper are i) to quantify sediment transport rates and processes across the different substrates; ii) to examine the evolution of near-bed turbulence from

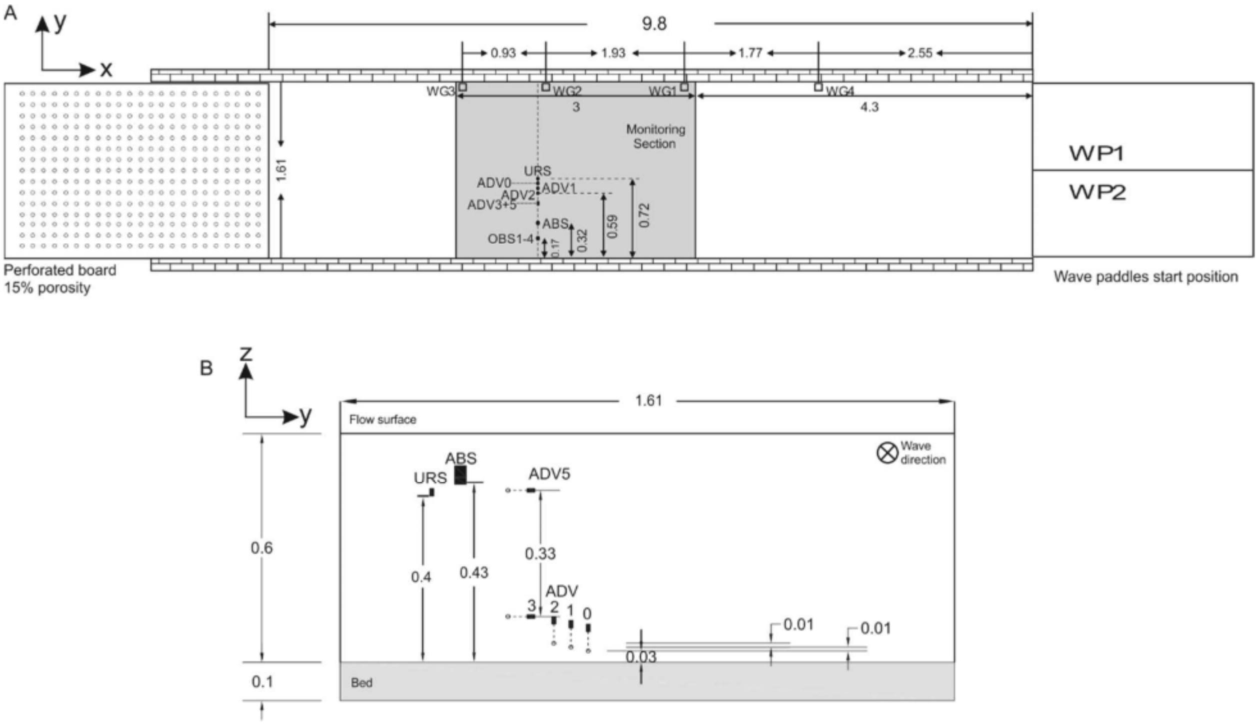

Figure 1. Plan view (A) and side view (B) of the experiment setup

the initial flat bed until ripple equilibrium morphologies are attained; iii) to find the relationship between initial bed clay fraction and rates of change in suspended sediment concentration through the experiments.

2 METHODOLOGY

Five large-scale flume experiments were conducted in the Total Environmental Simulator at the University of Hull, United Kingdom. The length and width of the tank are 9.8 m and 1.6 m, respectively, with a central monitoring section at a horizontal distance x=4.3 m from the wave generating paddles (Figure 1A). In the monitoring section, an acoustic backscatter system (ABS) is mounted at a distance x=6.1 m from wave generators and y=0.32 m from the flume wall (Figure 1A), which is 0.43 m above the bed (Figure 1B). Additionally, five SonTek acoustic Doppler velocimeters (ADV), aligning with the ABS, are positioned at five different heights (from 0.03 m to 0.36 m above the bed) to form a vertical array of measurements (Figure 1). Three of the ADVs are downward looking probes and two are sideward looking probes (Figure 1B). In line with the ABS and ADVs, there is a fixed ultrasonic ranging system (URS) for detecting ripple migration at distance y=0.72 m from the side wall (Figure 1A). At the end of the flume, there is a perforated board with a porosity of 15%, mounted at an upstream dipping angle of 6° (Figure 1A). The perforated board is to disperse wave energy and thus minimize wave reflections. The sediment bed in the flume was 0.1 m thick at the start of the experiments. All experiments used a mean water depth of 0.6 m and the salinity of the water was held constant in all runs at ca. 19 psu, which is typical for estuarine conditions. Experimental Run 1 used a bed of well-sorted sand with a median diameter of 496 µm. Wet kaolin clay, which is one of the most common clay types on Earth, was homogenously mixed with the same sand in Runs 3 to 6, with the initial clay fraction increasing from 4.2% to 7.4% (See Table 1 and Figure 2 in Wu et al., 2018). The experimental results of Run 02 that was conducted under irregular (polychromatic) wave are not discussed in this paper.

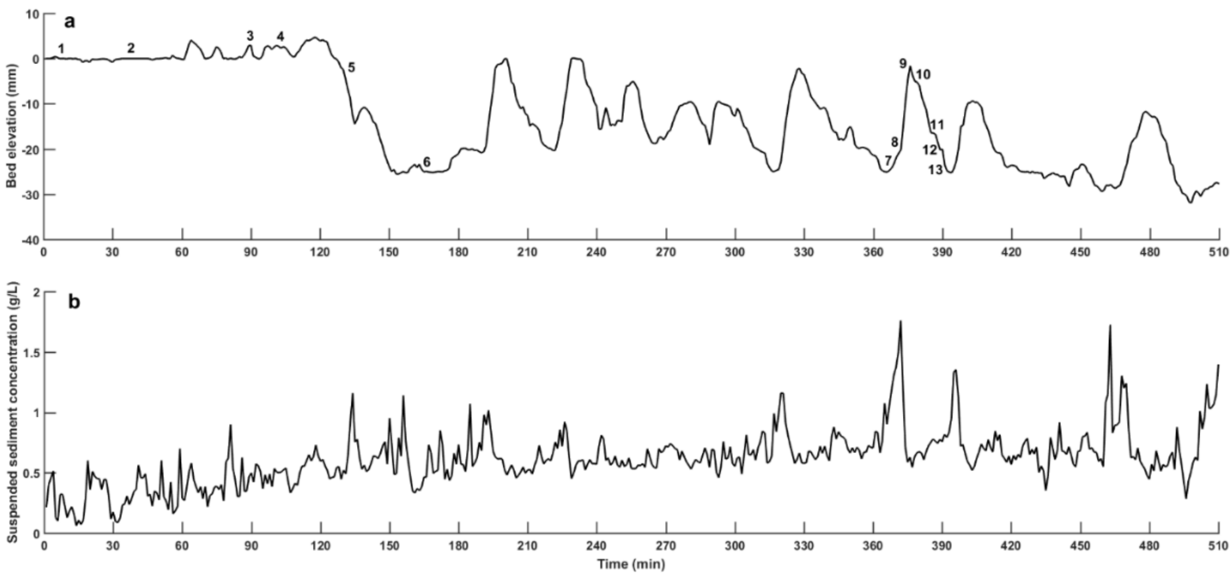

Figure 2. ABS detected bed elevation (a) and suspended sediment concentration (b) at 20 mm above the bed in Run 5 with 7.2% of initial bed clay fraction. The thirteen numbers of locations match numbered panels of phase averaged suspended sediment concentration field in Figure 3

3 RESULTS

3.1 Near-bed suspended sediment concentration (SSC)

3.1.1 Time averaged near-bed SSC

Representative example of suspended sediment concertation change over 20 mm above the bed with bedform development for Run 5 with the longest experimental duration of 510 mins is displayed in Figure 2. The bed was recorded to keep flat in the beginning 60 minutes. Over such a flat bed, the peak value of suspended sediment concentration (SSC) was about 0.7 g/L. However, the amount of suspended sediment was lower than 0.5 g/L at that time. With bed erosion, the SSC increased during the period between t = 60 min and t = 120 min. After that the bed elevation decreased significantly showing the formation of wave ripples. At the same time, there was an increase of the amount of suspended sediment, with maximum value of SSC exceeding 1 g/L. Then, ripple started to migrate beneath the ABS until the end of the experiment. Peak values of the SSC repeatedly appeared on the ripples lee sides, in particular with extremely high values, superior to 1.5 g/L after t = 350 min.

i. 3.1.2 Phase-averaged SSC

Figure 3 displays intrawave suspended sediment concentration field from 20 mm to 100 mm above bed, which equals to 4~5 ripple heights. The phase averaged velocity is also shown in the top left panel in Figure 3 to show the regular and asymmetrical wave. A wave period starts from peak value at phase angle as 0°. These contour plots reflect phase averaged intrawave SSC over 24 wave cycles. Over the flat bed in the beginning of experiment, the SSC field was characterized by laminar distribution gradually decreasing with height above 50 mm (Panel 1 to 3, Figure 3). At t = 105 min, this type of suspended sediment profile was broken by a suspended sediment cloud at a phase angle of 1.1 π rad (Panel 4, Figure 3). A larger suspended sediment cloud was observed just before the flow reached its maximum negative velocity per wave cycle, sediments expanding up over 70 mm height at t

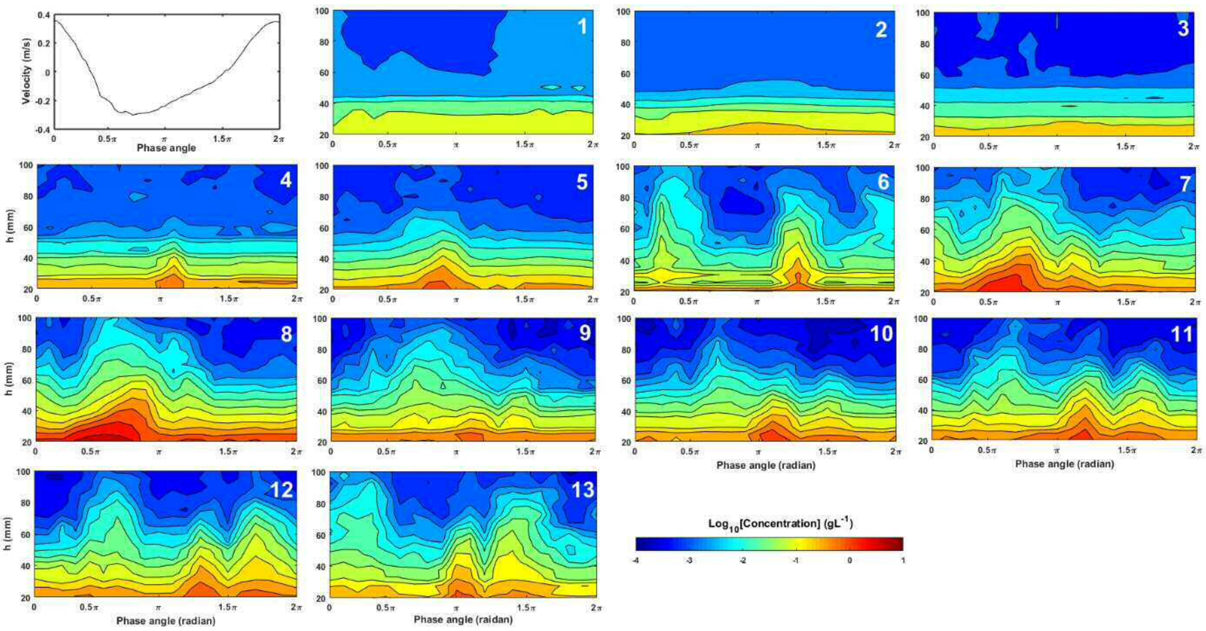

Figure 3. Wave velocity and phase averaged SSC profiles over the bed of Run 5 with 7.2% of initial bed clay fraction. The top left panel displays measured free stream velocity for over 24 successive wave periods. The thirteen numbered panels show phase-averaged suspended sediment concentration (SSC) for over 24 successive wave periods at respective time in Figure 2. The colours in the contour plots are defined in the colour bar as log_10[SSC]

= 130 min (Panel 5, Figure 3). It happened when the ripple was forming. The lamination of suspended sediment completely disappeared after t=160 min, with concentration peak appearing in each half of the wave cycle and suspending sediments up to nearly 90 mm height (Panel 6, Figure 3).

During the time between t =360 min and t =400 min, an equilibrium wave ripple moved under the ABS probe. At the lee side of wave ripple (number 7 and 8), a high concentration cloud appeared after flow reversal from positive to negative in the first half wave cycle, matching the peak SSC value in Figure 2b. The concentration peaks of smaller magnitude in the second half of wave period above locations 7 and 8 (Panel 7 and 8, Figure 3), were probably associated with the passage of an advected suspension cloud forming at neighboring downstream ripples. There were no noteworthy SSC peaks at ripple crest (locations 9 and 10). At locations 11 to 13 on the stoss slope of ripple, the SSC peaks in the first half wave cycle were presumably caused by the passage of an advected suspension cloud from successive upstream ripples. In the succeeding half cycle, the formation of concentration peaks occurred at a phase angle of more than 1.5 π rad was similar to that above lee side due to vortex shedding during flow reversal. The ones generated between phase angle of 1 π and 1.5 π were assumed to relate with sediment trapped within new generated vortices (Figure 3).

3.3 Ripple migration

Bedform elevation profiles detected by the fixed URS is shown in Figure 4, which demonstrates different ripple migration rates with different initial bed clay fraction. At the beginning of the control experiment (Run 1, pure sand), a wave ripple slowly moved beneath the URS probe between t = 20 min and t = 76 min (Figure 4), with the rate of around 0.04 mm/s. After t = 75 min, the mean migration rate increased to 0.14 mm/s with ripples reaching equilibrium.

In Run 3 with the lowest clay fraction of 4.2%, the bed was flat in the first 15

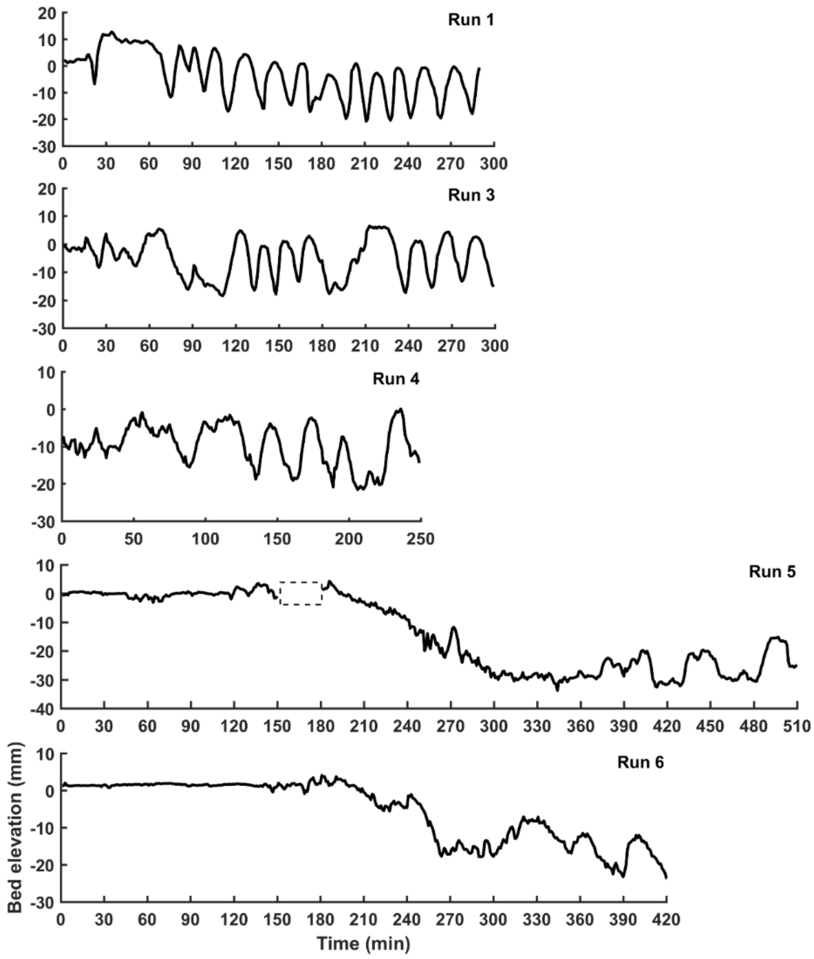

Figure 4. Bedform elevation profiles recorded by the fixed URS are used to determine wave ripple migration rate. The rectangle with dash line denotes data lost as technical problem of URS probe.

minutes, before ripple forming and starting to move. The fixed URS detected three migration of

small ripples with height smaller than 10 mm during period t = 15 min and t = 50 min (Figure 4). The mean migration rate after ripples developing to equilibrium (t > 60 min; Wu et al., 2018) is 0.11 mm/s. In the beginning of Run 4 (t < 40 min), there was only one small ripple movement detected. During time between t = 40 min and t = 140 min, the URS probe recorded two ripple movements (Figure 4). The ripple profiles had long flat crests, which indicates that ripple migration rate was relatively slow (Figure 4). However, the average migration rate increased notably from 0.04 mm/s to 0.1 mm/s in the following 2 hours, with four ripples migrating below the URS probe (Figure 4). Ripple migration rates for Run 5 and Run 6 with relatively higher initial clay fraction (7.4% and 7.6%, respectively) declined significantly. In Run 5, the bed elevation gradually decreased to around -30 mm during period between t = 180 min and t = 300 min. It possibly indicates a ripple trough forming beneath the URS probe during this time. Instead of larger ripple migration detected in the previous runs, there were three smaller ripples (η < 15 mm) moving in the last 150 minutes of the experiments (Figure 4). Similarly to Run 5, the bed below the URS probe in Run 6 experienced a significant decrease in approximately 100 minutes.

Additionally, there were only small size ripple migration recorded (Figure 4).

4 CONCLUSIONS

1. The suspended sediment concentration (SSC) field over the flat bed in each run was characterised by the lamination of suspended sediments, which immediately disappeared when the bed eroded. Several peak values of the SSC that related to vortices ejection and advection appeared in each wave cycle over both sides of wave ripples.

2. The time averaged SSC at height of 20 mm above the bed significantly increased from the flat bed evolving to equilibrium wave ripples.

3. The migration rate of wave ripples significantly decreased with an increase of the initial bed clay fraction.

5 ACKNOWLEDGEMENT

This work was part of the COHWAV project, supported by Seventh Framework Programme of 508 the European Community through a grant from the Integrating Activity HYDRALAB IV within the Transnational Access Activities programme, under contract no. 261520. The authors highly appreciate the help and advice from Aaron Westlake, Nick Coultish, Brendan Murphy, Kim Rosewell, Reinier Schrijvershof, and Leiping Ye during the setup and execution of the flume experiments.

6 REFERENCES

Green, M.O. & Black, K.P. 1999, Suspended-sediment reference concentration under waves: field observations and critical analysis of two predictive models, Coastal Engineering, vol. 38, no. 3, pp. 115-141.

Leeder, M. 2011, Sedimentology and sedimentary basins from turbulence to tectonics, 2nd edn, Wiley-Backwell, Noida.

Ikeda, S., Horikawa, K., Nakamura, H. & Noguchi, K. 1991, "Oscillatory boundary layer over a sand ripple model", Coastal Eng in Japan, vol. 32, pp. 15-29.

Nielsen, P. 1992, "Shear stress and sediment transport calculations for swash zone modelling", Coastal Engineering, vol. 45, no. 1, pp. 53-60.

O'Hara Murray, R., Thorne, P. & Hodgson, D. 2011, Intrawave observations of sediment entrainment processes above sand ripples under irregular waves, Journal of Geophysical Research: Oceans, vol. 116, no. C1.

Van der Werf, Jebbe J, Doucette, J., O'Donoghue, T. & Ribberink, J.S. 2007, Detailed measurements of velocities and suspended sand concentrations over full-scale ripples in regular oscillatory flow, Journal of Geophysical Research: Earth Surface, vol. 112, no. F2.

Wu, X., Baas, J. H., Parsons, D. R., Eggenhuisen, J., Amoudry, L., Cartigny, M., ... & Ruessink, G. 2018, Wave ripple development on mixed clay–sand substrates: Effects of clay winnowing and armoring. Journal of Geophysical Research: Earth Surface, vol. 123,pp. 2784-2801.